


Article

Laboratory Preparation and Performance Characterization of Steel Slag Ultrafine Powder Used in Cement-Based Materials

Yuanhang Sun ¹ , Meizhu Chen ^{1,2,*}, Dongyu Chen ¹, Shaoyan Liu ³, Xintao Zhang ¹ and Shaopeng Wu ¹

¹ State Key Laboratory of Silicate Materials for Architectures, Wuhan University of Technology, Wuhan 430070, China

² Wuhan University of Technology Chongqing Research Institute, Chongqing 401120, China

³ State Key Laboratory of Water Resources and Hydropower Engineering Science, Wuhan University, Wuhan 430072, China

* Correspondence: chenmzh@whut.edu.cn

Abstract: Steel slag is generally regarded as a supplementary cementitious material in cement-based materials, which is conducive to the realization of the goal of carbon peak and carbon neutralization. However, the lower cementitious activity and poorer volume stability of steel slag limit its high dosage in cement-based materials. In this paper, steel slag ultrafine powder (SSUP) was prepared in the laboratory through mechanical activation combined with grinding aids. Furthermore, the grinding time was optimized. The particle size, specific surface area, and microstructure characterization were evaluated for the SSUP compared with steel slag powder (SSP). The hydration properties of SSUP were studied by means of cement paste hydration heat and mortar strength. Meanwhile, the soundness of SSUP and SSP was compared by the Le chatelier soundness test. The process of preparing SSUP in the laboratory is as follows: the steel slag is ground by a horizontal ball mill for 50 min and then ground with a planetary ball mill mixing with the grinding aids for 15 min. The experimental results show that the hydration degree and rate of SSUP are better than that of SSP, and the activity index of SSUP is 94.19%, which is much higher than that of SSP (69.62%). The X-ray diffractometry (XRD) result shows that the content of the hydration products for SSUP is higher than that of SSP. The soundness test shows that the stability of SSUP is superior to that of SSP when the dosage is the same. Therefore, ultra-fining can effectively improve the cementitious activity and soundness of steel slag.

Keywords: cement-based materials; steel slag ultrafine powder; preparation; performance characterization



Citation: Sun, Y.; Chen, M.; Chen, D.; Liu, S.; Zhang, X.; Wu, S. Laboratory Preparation and Performance Characterization of Steel Slag Ultrafine Powder Used in Cement-Based Materials. *Sustainability* **2022**, *14*, 14951. <https://doi.org/10.3390/su142214951>

Academic Editor: Ning Yuan

Received: 17 October 2022

Accepted: 8 November 2022

Published: 11 November 2022

Publisher's Note: MDPI stays neutral with regard to jurisdictional claims in published maps and institutional affiliations.



Copyright: © 2022 by the authors. Licensee MDPI, Basel, Switzerland. This article is an open access article distributed under the terms and conditions of the Creative Commons Attribution (CC BY) license (<https://creativecommons.org/licenses/by/4.0/>).

1. Introduction

Cement, as a kind of inorganic cementitious material, is widely used in construction, water conservancy, road construction, and other projects because of the various areas in which it displays good performance. As a developing country, China is the world's largest cement producer and consumer. However, there are problems such as large consumption of primary resources and large emissions of waste gas and dust in the production of cement [1], which is not conducive to the development of dual carbon strategic objectives. Consequently, supplementary cementitious materials such as fly ash, silica fume, and slag are popular for replacing the part of cement [2–7] because the mineralogical phases of these industrial solid wastes are dicalcium silicate (C₂S), tricalcium silicate (C₃S), tricalcium aluminate (C₃A), and tetra calcium aluminoferrite (C₄AF), which are similar to those of cement [8,9].

Steel is the most versatile metal in the development of society, which results in its high production. Meanwhile, a huge amount of steel slag, which is the by-product in the steelmaking process, is generated. Nevertheless, the utilization rate of steel slag in China is only approximately 35% [10], resulting in large amounts of stockpiling and occupying a lot of land area. Using steel slag as a supplementary cementitious material can not only solve

the problem of environmental pollution, but also increase the utilization rate of steel slag, including decreasing the consumption of cement and ensuring the sustainable development of steel enterprises [11]. Nevertheless, the use of steel slag as a supplementary cementitious material must solve the problems of low cementitious activity and poor soundness because of the thermal history of steel slag [12–15].

There are three methods to improve the cementitious activity of steel slag, including physical, chemical, and thermal excitation. Physical excitation is the method used to reduce the steel slag's particle size by crushing, grinding, and so on, which can increase steel slag's specific surface area and cementitious activity [16–19]. Grinding can also destroy the crystal structure to promote the cementitious activity of steel slag. Chemical excitation activates the cementitious activity by adding chemical excitant [20]. Thermal excitation is the method used to change the structure of vitreous state in steel slag using a high temperature, which hydrates steel slag faster [21]. Among these three methods, physical excitation can not only promote the cementitious activity of steel slag, but also make the distribution of free calcium oxide (f-CaO) uniform, further improving the steel slag's soundness.

Some scholars have investigated the effect of grinding equipment on the specific surface area of steel slag powder (SSP). Moreover, they have also researched the relationship between the cementitious activity and particle size of SSP. Li X. et al. [22] investigated the relationship between the specific surface area of SSP and the ball/raw steel slag ratio (b/r). They found that a b/r of 5/1 is the best condition for milling the SSP. However, the SSP prepared by them still does not meet the standard of SSUP requiring that the specific surface area is greater than 700 m²/kg and the residue on the 30 μm sieve is less than 1%, while the particle size of D15 is less than 3 μm, that of D50 is less than 10 μm, and that of D90 is less than 30 μm. Zhu X. et al. [17] found that alcohol grinding aids could increase the specific surface area of SSP from 246.9 m²/kg to 354.5 m²/kg. Wang Q. et al. [2] prepare steel slag ultrafine powder (SSUP) with a specific surface area of 786 m²/kg by mechanical grinding. They found that SSUP exhibits a higher activity at an early and middle age. At the age of 3 d, the activity index of SSP is only 35.9%, which is much lower than that of SSUP. At the age of 28 d, the activity index of SSUP reaches 72.8%, which is close to that of SSP at 360 d. However, they did not come up with a specific method for preparing SSUP.

The current research only provides the relationship between the particle size and the cementitious activity of SSP. However, there is little research into the relationship between the granularity and soundness of SSP. Besides, there are a few studies on the preparation of SSUP in a laboratory. Therefore, the research focus of this paper is a new laboratory method for preparing SSUP. The SSUP was prepared firstly with a horizontal ball mill and was then milled by a planetary ball mill, combining the grinding aids. Then, the soundness and cementitious activity of cement-based materials with SSUP were measured by Le chatelier soundness test, X-ray diffractometry (XRD), and strength and hydration heat test. The experimental flow chart is shown in Figure 1.

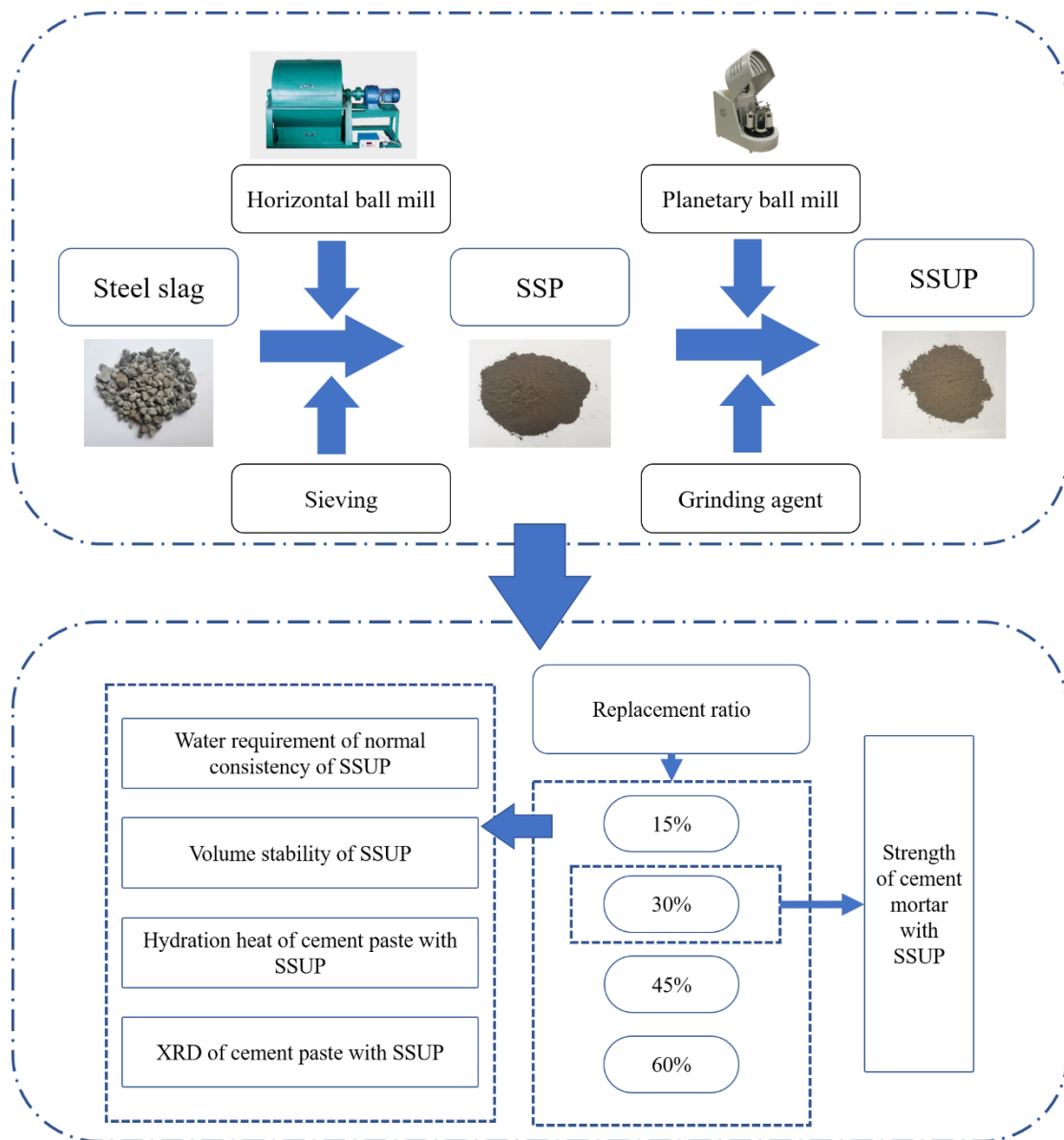


Figure 1. Experimental flow chart.

2. Materials and Experimental Methods

2.1. Raw Materials

P·O 42.5 Portland cement used in this study was produced by Anhui Conch Cement Limited Company of China. Hot disintegration steel slag used in the experiment was collected from Baowu Group of China. The chemical compositions of steel slag and Portland cement selected for this test are listed in Table 1, and were tested by X-ray fluorescence (XRF). The basic performances of cement are listed in Table 2. As can be seen from Table 1, the main oxides of steel slag are CaO, Fe₂O₃, SiO₂, Al₂O₃, and MgO, which are similar to Portland cement. The main difference is that the steel slag is generated by steelmaking, which results in its Fe₂O₃ content being much higher than that of cement containing only 3.27% Fe₂O₃. Based on the chemical compositions, the basicity of the steel slag can be calculated from Equation (1) as follows. According to the basicity, steel slag is often divided into three types, namely, high basicity slag, medium basicity slag, and low basicity slag, and the specific classification is shown in Table 3.

$$R = \frac{m_{CaO}}{m_{SiO_2} + m_{P_2O_5}} \quad (1)$$

Table 1. Chemical compositions of steel slag and cement used in this study.

Chemical Composition (%)	CaO	Fe ₂ O ₃	SiO ₂	MgO	Mn ₃ O ₄	Al ₂ O ₃	P ₂ O ₅	TiO ₂	SO ₃	LOI	Others
steel slag	38.30	28.61	13.68	6.21	4.29	2.86	2.02	1.25	0.36	1.03	0.69
cement	50.57	3.27	25.38	4.48	0.15	8.02	0.12	0.52	2.95	3.32	1.22

Table 2. Basic physical properties of cement used in this study.

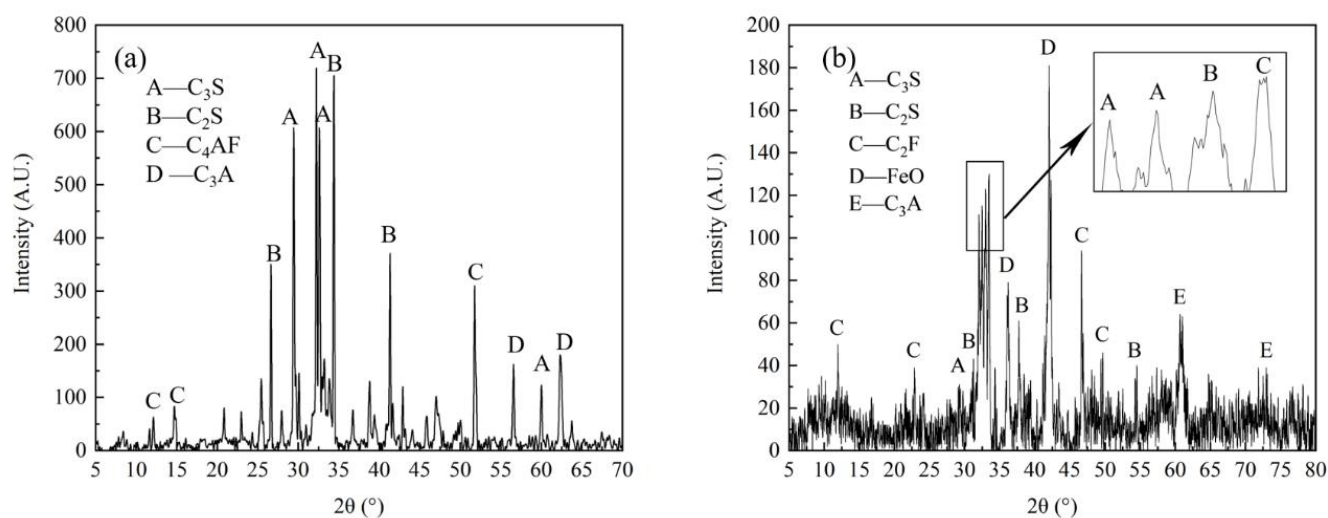
Specific Surface Area (m ² /g)	Compressive Strength (Mpa)		Flexural Strength (Mpa)		Setting Time (Min)	
	7 d	28 d	7 d	28 d	Initial	Final
1.68	31.17	43.28	6.20	8.53	52	563

Table 3. Classification of steel slag by basicity.

Species of Steel Slag	Basicity
high basicity slag	$R < 1.8$
medium basicity slag	$1.8 < R < 2.5$
low basicity slag	$R > 2.5$

Calculated from Equation (1), the basicity of steel slag used this study is 2.86, which is higher than 2.5. This means that this kind of steel slag belongs to the category of high basicity slag, and it is known that its main mineralogical phases are C₂S, C₃S, C₃A, and dicalcium ferrite (C₂F), which are similar to those of cement. Therefore, this kind of steel slag theoretically has good cementitious activity.

The mineralogical phases of cement and steel slag are shown in Figure 2, and were measured by XRD. As can be seen from Figure 2, the main mineralogical phases of cement and steel slag are C₃S, C₂S, and C₃A. Besides, iron element mainly exists in the form of C₂F in steel slag and C₄AF in cement, which is due to the high content of iron oxide in steel slag. Consequently, steel slag has certain cementitious activity and can be used as a cementitious material [23]. However, the cementitious activity of steel slag is lower than that of Portland cement, because the content of C₃S in steel slag is not only lower than that of C₃S in Portland cement, but also lower than that of C₂S in steel slag. Meanwhile, the early strength of cement concrete is mainly provided by C₃S, while the later strength is mainly provided by C₂S. Therefore, the early strength provided by SSP is low, but the later strength provided by SSP is high.

**Figure 2.** Mineralogical phases of cement and steel slag: (a) cement and (b) SSP.

2.2. Laboratory Preparation of SSUP

The process of preparing SSUP in this experiment is shown in Figure 1. The function of the horizontal ball mill is to grind steel slag into steel slag powder. Then, the particle size of SSP is further reduced by the planetary ball mill to prepare SSUP. The SSP after grinding was sieved by 0.075 mm. Then, the laser particle size analyzer was used to test the particle size of SSP to confirm the optimum initial grinding time. The SSP after grinding for the optimum initial grinding time was mixed with the grinding aids to investigate its effect on grinding and then ground by a planetary ball mill. Following this, the particle size and specific surface area of SSP were tested to confirm the optimum regrinding time.

2.3. Experimental Methods

2.3.1. Laser Particle Size Analyzer

The particle size of SSUP and SSP was determined using a Mastersizer 2000 Laser particle size analyzer with ethanol as a dispersant at a sampling rate of 1000 times/s, and the refractive index of the mixture was set to 1.52.

2.3.2. Automatic Specific Surface Area and Pore Analyzer

The specific surface area of SSUP and SSP was measured by a fully automatic specific surface area and pore analyzer ASAP 2460. The samples were pretreated by drying at 100 °C for 4 h and setting to degas at 150 °C for 10 h.

2.3.3. Scanning Electron Microscope

The microstructures of SSUP and SSP were analyzed by backscattered electron images using a JSM-IT300 scanning electron microscope with an attached X-MaxN20. The powder needs to be gold plated before testing owing to the poor electrical conductivity of steel slag. The difference between SSUP and SSP was judged by micromorphological analysis.

2.3.4. Water Requirement of Normal Consistency of Cement Paste with SSUP

The water requirement of the normal consistency of cement pastes with SSUP or SSP should be investigated firstly according to the GB/T 1346-2011 by the Vicat apparatus. The mass ratio of SSUP to cement was 15%, 30%, 45%, and 60% in this study. Then, the water requirement of normal consistency compared with SSP was measured.

2.3.5. Volume Stability of Cement Paste with SSUP

The volume stability of SSUP compared with SSP was tested in accordance with the GB/T 1346-2011. Ma [24] found that, when the dosage of SSP is lower than 50%, the soundness of cement-based material is qualified. Meanwhile, the soundness of paste with SSUP was superior to that with SSP. Consequently, the mass ratio of SSUP to cement was 15%, 30%, 45%, and 60% in this study. Then, the soundness of cement paste with SSUP compared with SSP was measured.

2.3.6. Isothermal Calorimetry of Cement Paste with SSUP

The hydration heat of cement paste with SSUP was tested by a TAM Air isothermal calorimeter at 20 ± 0.02 °C. The substitution rate of SSUP for cement was 15%, 30%, 45%, and 60%, respectively. The water to binder mass ratio was 0.5. The control sample was prepared using cement paste with the same dosage. Meanwhile, the difference between SSUP and SSP was also analyzed for the hydration heat in order to demonstrate the surface area of SSP on its hydration. The mix proportions of these samples are shown in Table 4.

Table 4. Mix proportions of different samples used in hydration heat.

Samples	Cement (g)	SSP (g)	SSUP (g)	Water (g)
C	10.0	/	/	5
A1	8.5	1.5	/	5
A2	7.0	3.0	/	5
A3	5.5	4.5	/	5
A4	4.0	6.0	/	5
B1	8.5	/	1.5	5
B2	7.0	/	3.0	5
B3	5.5	/	4.5	5
B4	4.0	/	6.0	5

2.3.7. Strength of Cement Mortar with SSUP

The compressive and flexural strengths of cement mortars with SSUP were measured in accordance with the GB/T 17671-2020. To prepare the testing samples (size: 40 × 40 × 160 mm), the Portland cement was mixed with SSUP in the proportion of 7:3 and the water to binder ratio was 0.5. Meanwhile, the difference between SSUP and SSP was also analyzed. Besides, the control sample was prepared using cement mortar with the same dosage. The compressive and flexural strengths of the samples under different curing times (7 and 28 days) were tested. The mix proportions of these samples are shown in Table 5.

Table 5. Mix proportions of different samples used in compressive and flexural strengths.

Samples	Cement (g)	SSP (g)	SSUP (g)	ISO Standard Sand (g)	Water (g)
P-O	450	/	/	1350	225
SSP	315	135	/	1350	225
SSUP	315	/	135	1350	225

2.3.8. X-ray Diffractometry of Cement Paste with SSUP

The hydration products of cement pastes with SSUP compared with SSP were tested by XRD to compare the hydration degree between them. Cement paste samples were prepared, which were cured for 3 d, 7 d, and 28 d, respectively. The mixed proportions of cement pastes are shown in Table 6.

Table 6. Mix proportions for hydration products testing.

Types of Gelling Material	Cement (g)	SSP (g)	SSUP (g)	Water (mL)
SSP	315	135	/	112.5
SSUP	315	/	135	112.5

3. Results and Discussion

3.1. Influence of Preparation Process on Particle Size of SSUP

The particle size after grinding is related to the grinding time. In order to define the optimum initial grinding time, the steel slag is added to the horizontal ball mill for grinding for 45, 50, 55, 60, 65, and 70 min, respectively. Then, a laser particle size analyzer is used to test the particle size of steel slag. The results are shown in Figure 3, where it can be seen that, with the increase in grinding time, the D15, D50, and D90 particle sizes of SSP show a trend of decreasing first and then increasing. This is because the work of grinding media on steel slag increases with the increase in the grinding time. However, when the time continues to increase, the crushed steel slag generates a new surface, which has a high surface energy and results in a strong adsorption capacity, leading to a greater particle size of steel slag. Therefore, the grinding time has an optimal value where the particle size of SSP reaches the minimum value. It can be seen from Figure 3 that the optimal grinding time is 50 min.

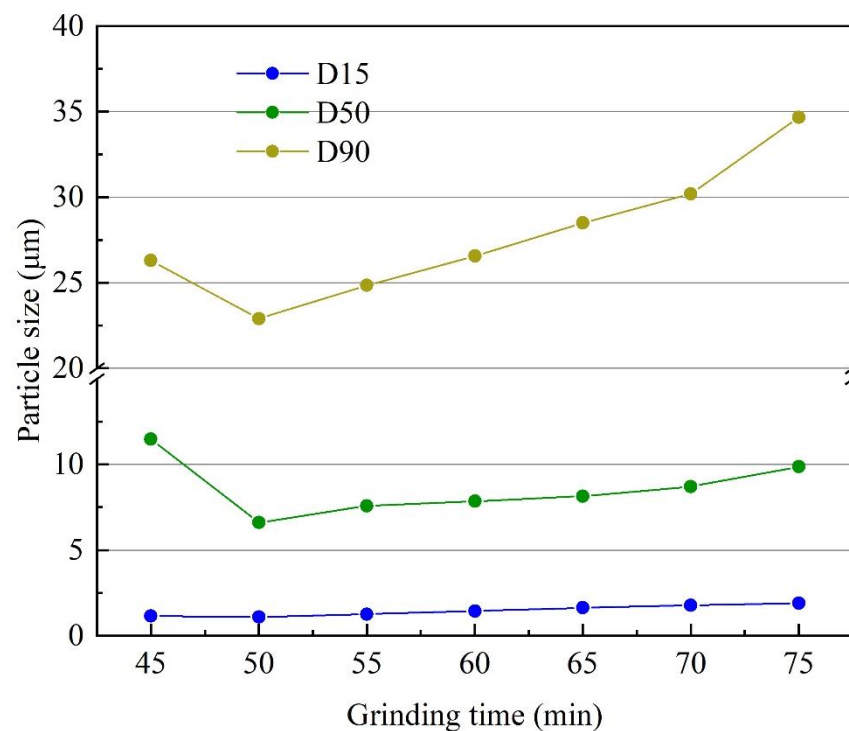


Figure 3. Influence of grinding time on the particle size of SSP.

It is still necessary to regrind the SSP because the residue on the 30 µm sieve of the SSP is 7.28% after grinding for 50 min, which is still higher than the standard 1% of SSUP. The SSP after grinding for 50 min is divided into eight groups and milled for 5, 10, 15, and 20 min, respectively, by a planetary ball mill. Meanwhile, the influence of the grinding aids on the particle size of SSP after regrinding is discussed. The experimental groups are shown in Table 7. The grinding aid is a solution of ethylene glycol, triethanolamine, and anhydrous ethanol with a volume ratio of 1:1:1, and the steel slag to grinding aids ratio is 75 g to 1 mL [25].

Table 7. Experimental groups of steel slag regrinding.

Samples	A I	A II	B I	B II	C I	C II	D I	D II
Regrinding time (min)	5	5	10	10	15	15	20	20
Grinding aids	/	√	/	√	/	√	/	√

The results of eight groups of regrinding SSP tested by a laser particle size analyzer are shown in Figures 4–6. It can be seen that, when the grinding time is the same, the D15, D50, and D90 particle sizes of samples with grinding aids are smaller than those without grinding aids. This means that the grinding aids can improve the grinding effect and effectively decrease the particle size of steel slag after grinding. When the grinding aids are added, with the increase in grinding time, the D15, D50, and D90 particle sizes of SSP show a trend of decreasing first and then increasing. In 15 min, the particle sizes reach the minimum value; therefore, the optimal time of regrinding is determined to be 50 min.

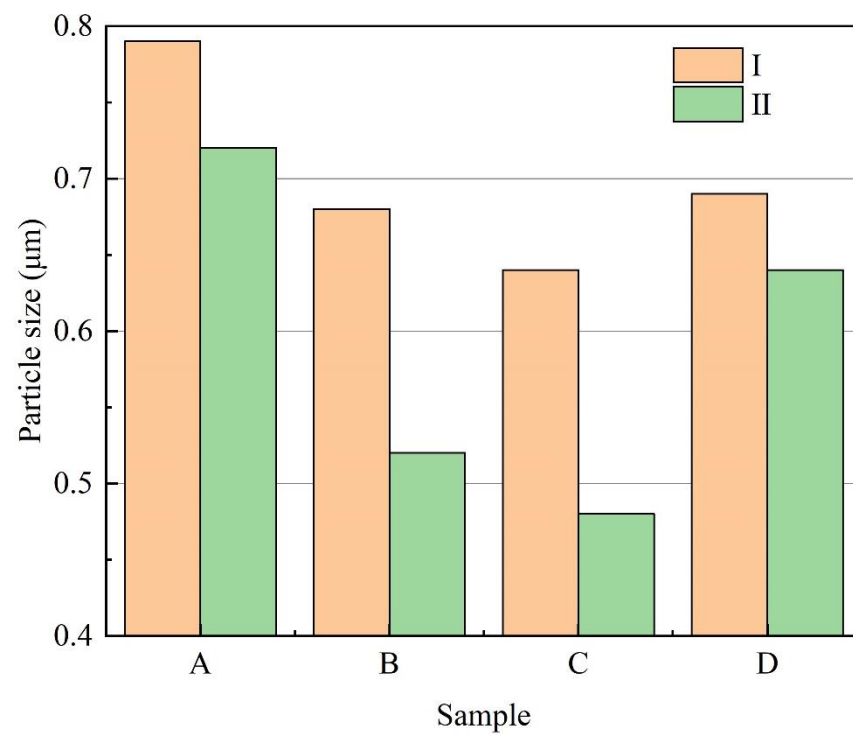


Figure 4. Influence of regrinding time and grinding aids on the D15 particle size of SSP.

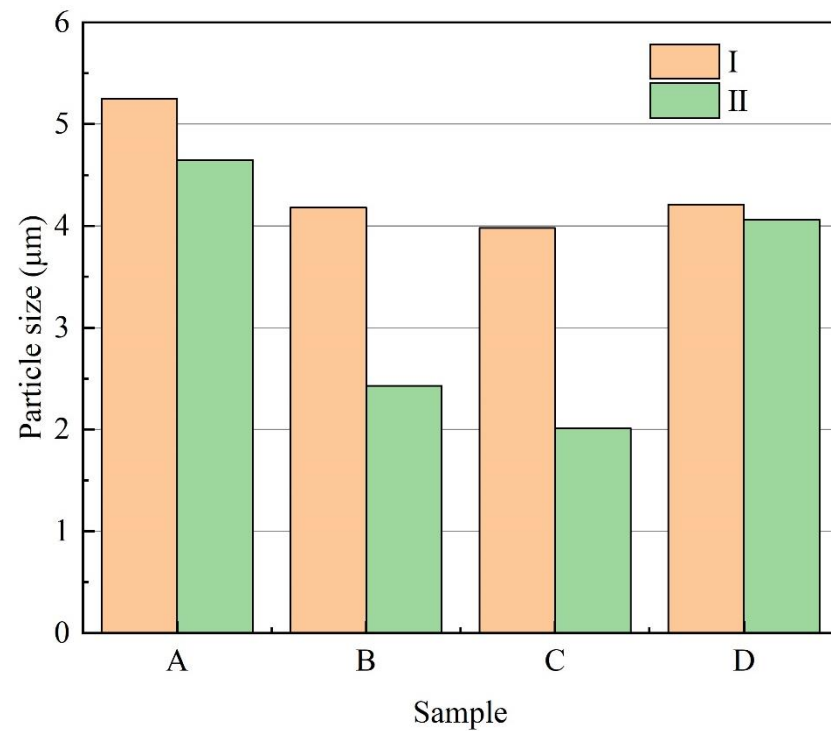


Figure 5. Influence of regrinding time and grinding aids on the D50 particle size of SSP.

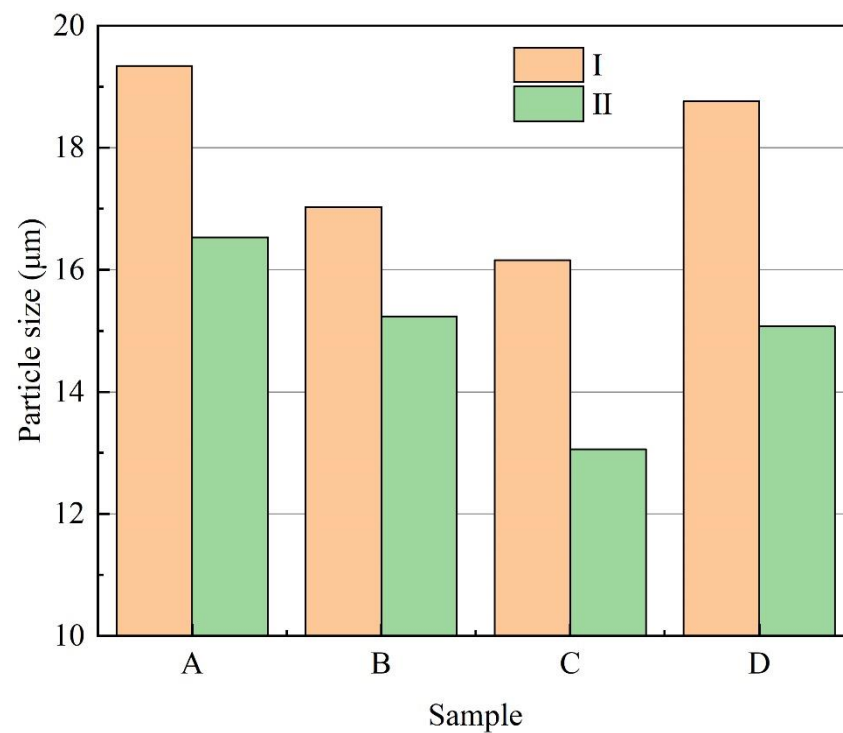


Figure 6. Influence of regrinding time and grinding aids on the D90 particle size of SSP.

According to the results of the laser particle size analyzer, the particle sizes of D15, D50, and D90 of SSP that is reground for 15 min are 0.48 μm , 2.03 μm , and 12.19 μm , respectively, and the particle sizes of D15, D50, and D90 of SSP that is only ground for 50 min are 0.875 μm , 9.078 μm , and 32.419 μm , respectively. This shows that regrinding can effectively reduce the particle size of SSP. In addition, the experimental result of graded percentage retained is shown in Figure 7. It can be seen that the particle size distribution of SSUP is mainly around 1 μm compared with the SSP, which is smaller than that of the control group.

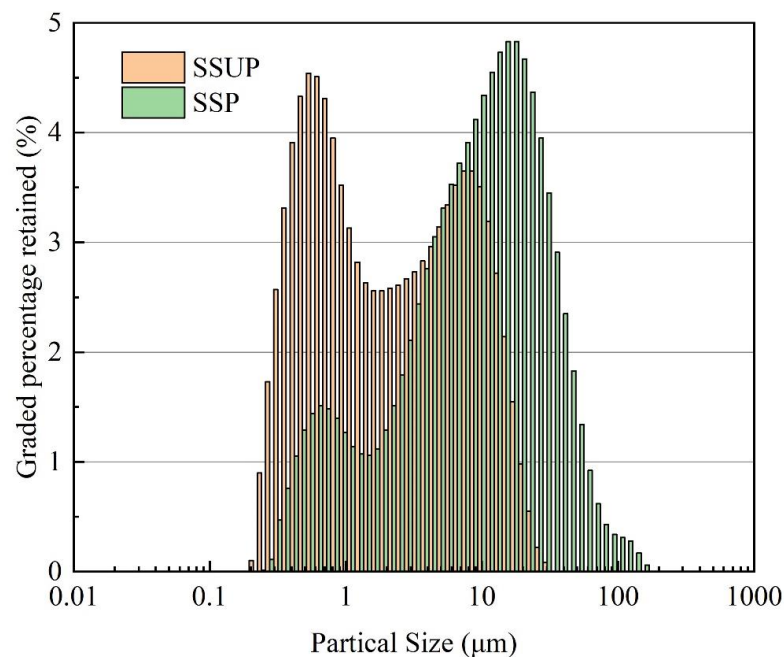


Figure 7. Comparison of graded percentage retained between SSUP and SSP.

The specific surface area of SSP reground for 15 min is measured by Brunauer–Emmett–Teller (BET) specific surface area analysis and laser particle size analysis. It shows that the BET of SSP reground for 15 min is $4.13 \text{ m}^2/\text{g}$ and that of SSP that is only milled for 50 min is only $2.13 \text{ m}^2/\text{g}$. All of the results meet the criteria of SSUP, which means that SSUP can be prepared by grinding for 50 min by a horizontal ball mill and then regrinding for 15 min by a planetary ball mill combining the grinding aids.

3.2. Microstructure of SSUP

The microstructures of SSUP and SSP at different magnifications of the scanning electron microscope are shown in Figure 8, with magnifications of 500, 1000, 2000, and 5000, respectively. It can be seen from Figure 8 that SSUP has a smaller particle size and its particle size is distributed more uniformly compared with SSP. When the magnification is 500, the surface of SSP's large particles is rougher. However, when the magnification is larger, the surface smoothness of SSUP and SSP is similar, even the surface of SSP is smoother. This is because, when the magnification is 500, SSP contains larger particles, and these large particles are not sufficiently ground, so the surface is rougher. When the magnification is larger, the observed SSPs are similar in size to SSUP, but the ultra-fine treatment of steel slag will cause crystal defects such as dislocation, making its surface rougher than the surface of micronized powder, which is conducive to improving the activity of SSUP, increasing its hydration reaction activity.

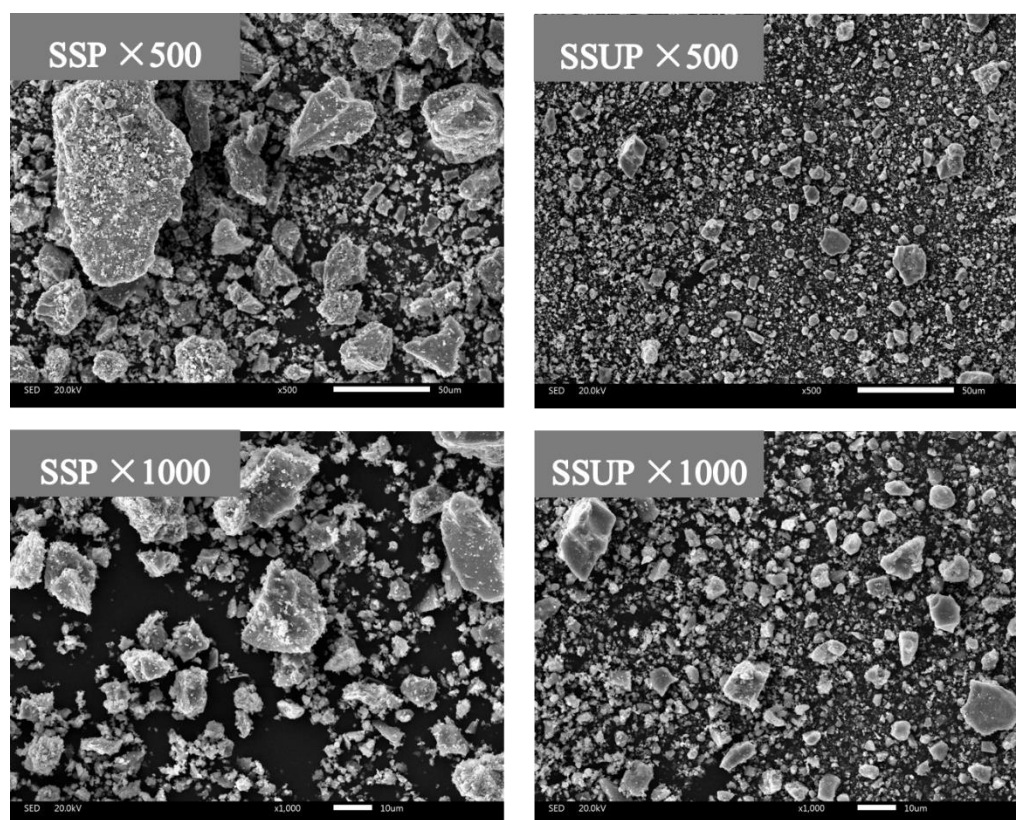


Figure 8. Cont.

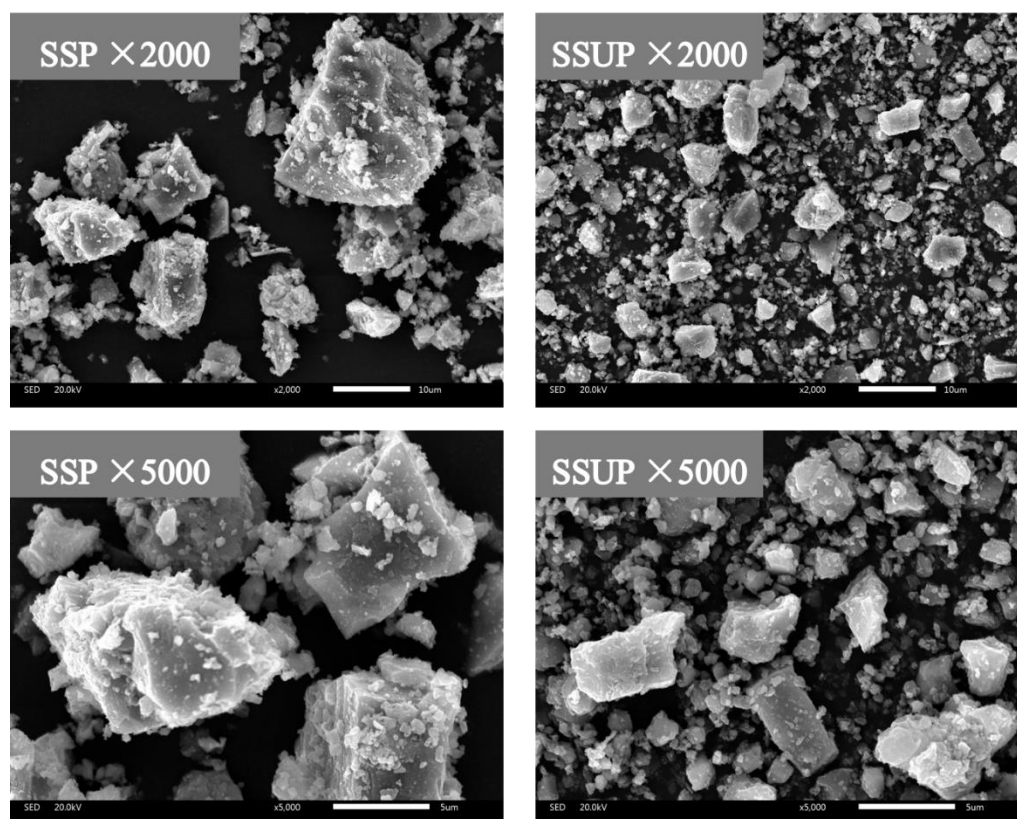


Figure 8. SEM images of SSUP and SSP (left: SSP, right: SSUP).

3.3. Water Requirement of Normal Consistency

The cement is displaced by SSUP at 15%, 30%, 45%, and 60% replacement weight ratios. Meanwhile, the difference between SSUP and SSP was also analyzed. The water requirements of normal consistency of cement paste with SSUP or SSP are shown in Figure 9. It can be seen that the water requirement of normal consistency for the samples with SSUP or SSP shows a decreasing trend when the replacement ratio is gradually increased. This is because both SSUP and SSP are small particles with smooth surfaces and have a morphological effect, which can improve the fluidity of the paste and, therefore, have the effect of water reduction. As a result, the water consumption decreases with the increase in the replacement ratio.

The water requirement of normal consistency of the samples with SSP is higher than that of the samples with SSUP when the dosage is 15% and 30% because of its larger partial size. SSUP has a better morphological effect, which can reduce the water consumption. However, when the dosage is further increased, the water consumption of SSUP is greater than that of SSP. This is because the specific surface area of SSUP is much higher than that of SSP, more water is needed to wrap the particles, which leads to a higher water requirement of normal consistency. In addition, most of the non-spherical SSUPs are not compacted and packed. As the particle size decreases, more voids appear among the particles. It also requires more water to fill the gaps among the different particles. Therefore, the amount of water required to maintain normal consistency is increased [26]. Further, the reaction is more rapid and the degree of hydration is higher at the same time, because the cementitious activity of SSUP is higher than that of SSP. The above reasons lead to high water consumption of SSUP.

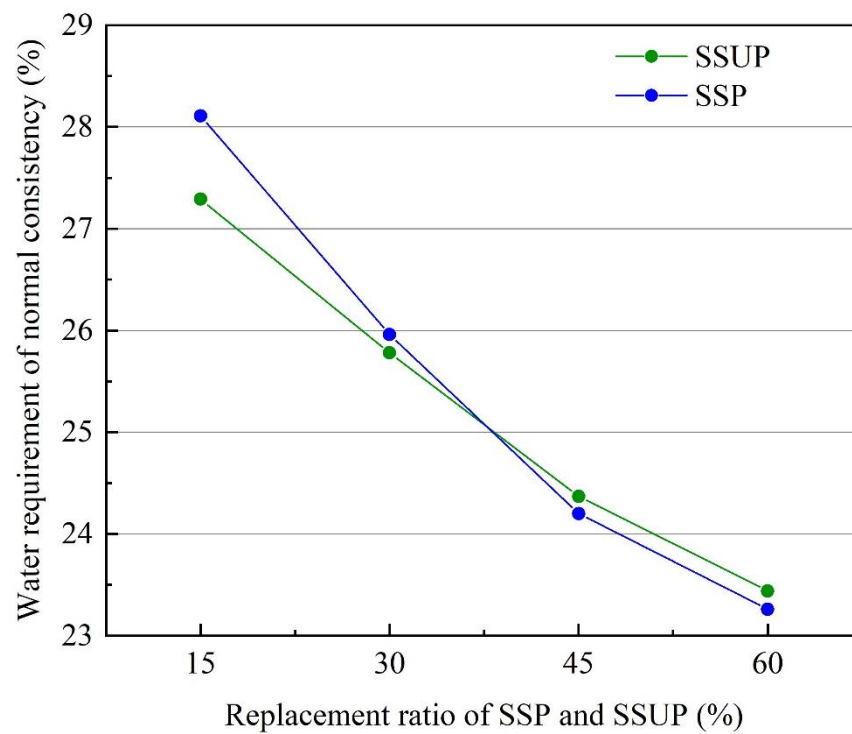


Figure 9. Water requirement of normal consistency at different dosages of SSUP and SSP.

3.4. Soundness of SSUP

The soundness of SSUP is tested by the Le chatelier soundness test after replacing 15%, 30%, 45%, and 60% of cement, respectively. Meanwhile, the difference between SSUP and SSP is also analyzed. The distance from the tip of the pointer represents the volume expansion rate of the samples and the results are shown in Figure 10.

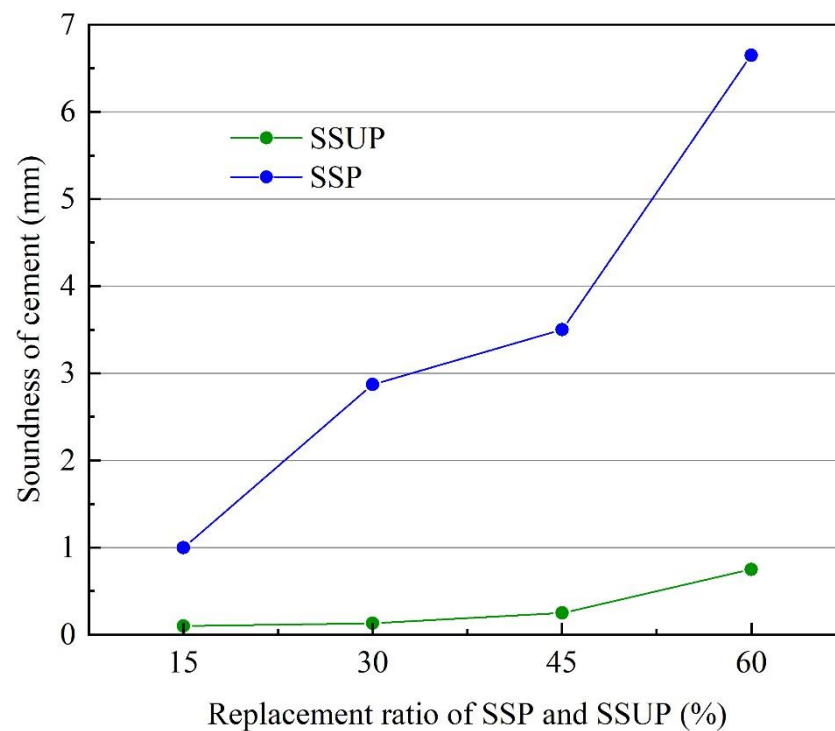


Figure 10. Influence of different SSUP and SSP replacement ratios on the soundness.

The volume expansion of steel slag is mainly due to the f-CaO. The f-CaO can react with water and generate $\text{Ca}(\text{OH})_2$, which results in 97.8% volume expansion [27]. Meanwhile, the hydration speed of the f-CaO is slower than that of C_3S and C_2S . This means that the volume expansion of the f-CaO occurs when the cement paste hardens, which can be detrimental to the volume stability of the cement-based material.

As can be seen from Figure 10, with the increase in the content of SSUP and SSP, the difference in the distance between the tip of the Lehigh clamp pointer before and after boiling gradually increases, and the difference in SSP is greater than the difference in SSUP at the same replacement ratio. When the dosage increased from 15% to 60%, the difference in SSUP increased from 0.10 mm to 0.75 mm, while the difference in SSP increased from 1.00 mm to 6.65 mm. This is because of the f-CaO and free magnesium oxide (f-MgO) contained in the steel slag, which will undergo volume expansion when hydrated, with a volume expansion rate as high as 90% to 100%. This causes volume expansion of the cement paste and, consequently, degradation of the soundness of cement. In conclusion, ultra-fining can effectively optimize the soundness of steel slag.

3.5. Hydration Heat of Cement Paste with SSUP

Figure 11 shows the isothermal calorimetry of cement paste with different dosages of SSUP compared with SSP. In Figure 11a, there is a major hydration peak followed by a second hydration peak, corresponding to the reaction of C_3A and C_2S , respectively. When the second peak appears, the hydration reaction enters the acceleration period. It can be seen that, with the increase in the dosages of SSUP and SSP, the peak area decreases because of the weak hydration ability of SSUP and SSP compared with cement. Besides, the peak area of SSUP is larger than that of SSP at the same dosage, which shows that the hydration rate of cement paste with SSUP is faster than that of samples with SSP. In terms of cumulative heat, each group has two exothermic stages. However, the second exothermic stage of the group with SSP is relatively small compared with that of the others. Besides, with the increase in dosages of SSUP and SSP, the cumulative heat decreases. This is because the hydration ability of SSUP and SSP is weaker than that of cement. When the dosage is same, the cumulative heat of paste with SSUP is larger than that with SSP and the second peak of SSUP appears earlier. These prove that the hydration ability of SSUP is stronger than that of SSP.

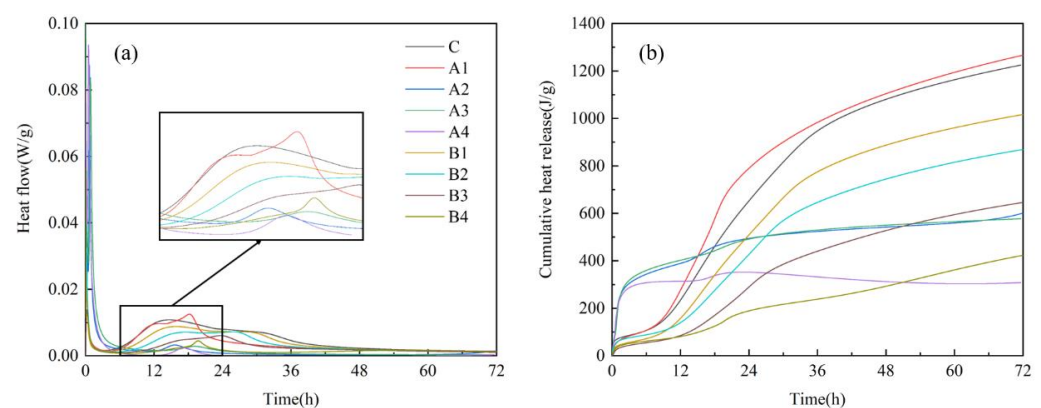


Figure 11. Hydration heat of cement paste with different dosages of SSUP and SSP: (a) heat flow and (b) cumulative heat.

3.6. Cementitious Activity of SSUP

The results of cementitious activity of SSUP measured in accordance with the GB/T 17671–2020 are shown in Figures 12 and 13. Meanwhile, the difference between SSUP and SSP was also analyzed. It can be seen that the flexural and compressive strengths of samples with SSUP or SSP increase with time. The flexural and compressive strengths of the control sample without steel slag powder are the largest when the curing time is

the same, followed by SSUP, and the lowest strength of SSP. This is because of the higher content of C_3S in cement compared with steel slag, which can provide greater hydration strength. In addition, the particle size of SSUP is smaller than that of SSP because of grinding. The specific surface increases with the decrease in particle size. This results in a more complete hydration reaction and a higher strength. However, the growth rates of flexural and compressive strength are both highest for SSUP, reaching 41.87% and 98.87%, respectively; followed by SSP, at 38.82% and 84.81%, respectively; and the lowest for cement, at 37.58% and 35.96%, respectively. This is because the C_2S content in steel slag is higher than the C_2S content in cement and C_2S hydrates slowly and mainly provides later strength, so the later strength growth rate of steel slag is higher than that of cement.

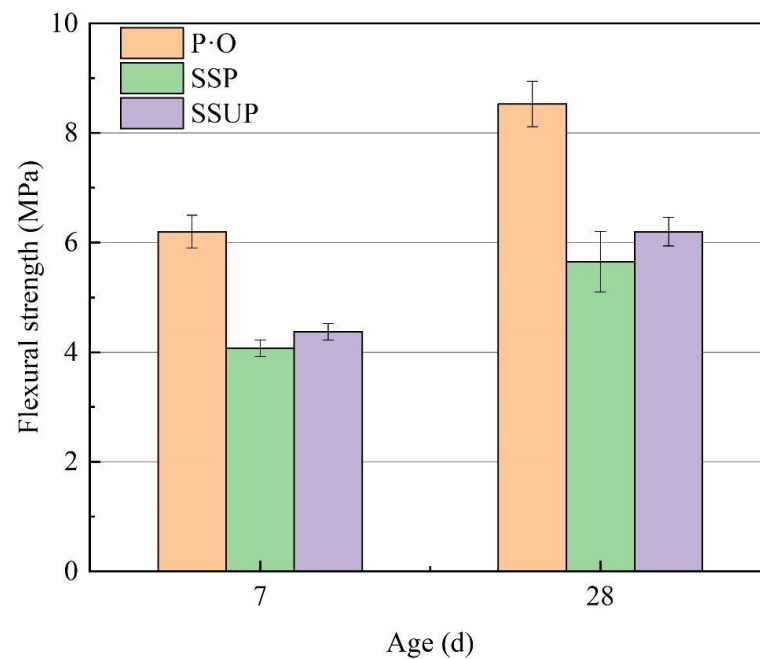


Figure 12. Flexural strength of Portland cement, SSUP, and SSP at 7 and 28 days.

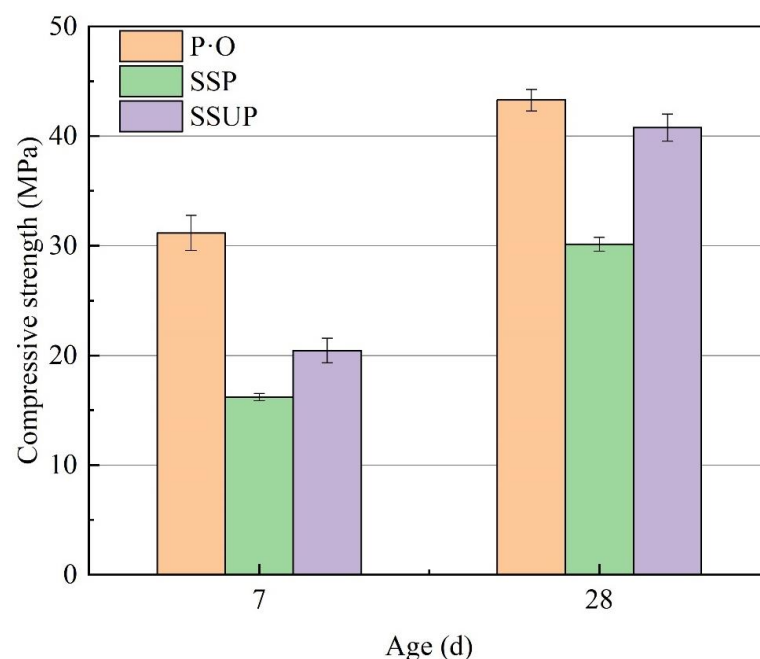


Figure 13. Compressive strength of Portland cement, SSUP, and SSP at 7 and 28 days.

The activity index is the ratio of the compressive strength between the test sample and the comparison sample, which can evaluate the cementitious activity of SSUP and SSP. The activity index was calculated using Equation (2).

$$A = \frac{R_t}{R_o} \times 100\% \quad (2)$$

where A [%] is the strength activity index of SSUP and SSP. R_t [MPa] is the compressive strength of the samples with SSUP or SSP. R_o [MPa] is the compressive strength of the control sample without SSUP or SSP.

As can be seen from Figure 14, the activity index of both SSUP and SSP increased with time. At 7 d, the activity index of SSUP is 65.61%, 13.63% higher than that of SSP. At 28 d, the activity index of SSUP is 94.19%, 24.57% higher than that of SSP. This is because grinding, as a physical excitation method, can lessen the particle size of steel slag, enhance its specific surface area, destroy the physical phase structure and the intact crystal structure of steel slag, and consequently improve its cementitious activity. In addition, the particle size of SSUP is smaller, which enables SSUP to better fill pores and makes the structure more compact. For the above reasons, the strength of cement mixed with SSUP is higher than that of cement mixed with SSP.

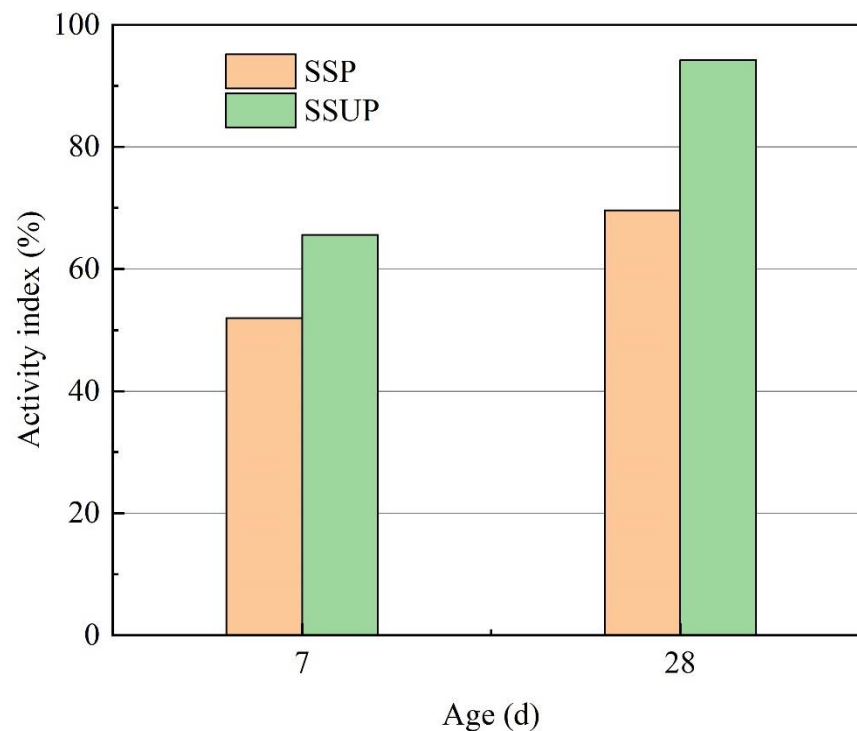


Figure 14. Activity index of SSUP and SSP at 7 and 28 days.

3.7. Hydration Products of SSUP

The XRD test results of cement paste with SSUP compared with SSP are shown in Figure 15. The phase composition includes calcium hydroxide crystal (CH) and C_3S , C_2S , C_3A , and C_2F , which are not hydrated completely. The hydration product, calcium silicate hydrate (C-S-H) gel, cannot be detected because of the principle of XRD. To compare the hydration degree of SSUP and SSP, the reductions in C_3S , C_2S , C_3A , and C_2F are used to delegate the increase in C-S-H gel [28,29].

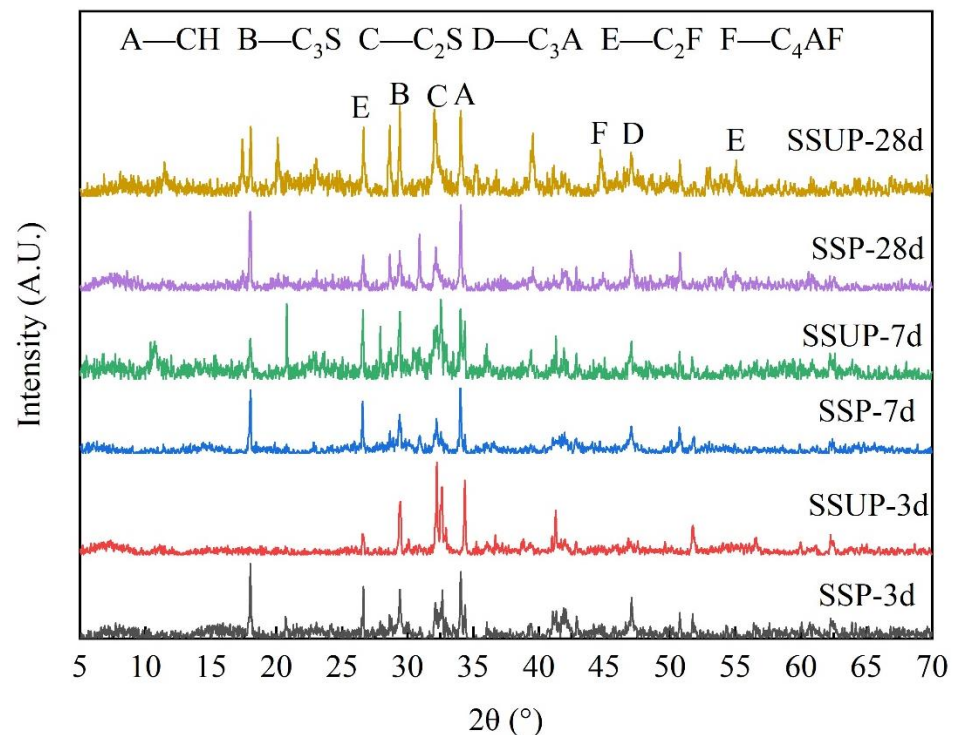


Figure 15. Mineralogical phases of cement paste with SSUP and SSP.

It is shown that, with the increase in time, the relative amounts of C_3S , C_2S , C_3A , and C_2F in SSP gradually decrease, but the degree of decrease is minor. However, although the relative amounts in SSUP have the same trend, the degree of decrease is large. This means that the relative amount of C-S-H gel in cement pastes with SSUP is larger than that in the samples with SSP. This is because the specific surface area of SSUP is larger, which means that the interface between steel slag and water is larger and the hydrate reaction rate is higher when the total mass of SSUP and SSP is the same. This indicates that both SSUP and SSP have taken place in a hydration reaction, while the hydration degree of SSUP is larger than that of SSP. This proves that ultra-fining can improve the hydration degree of steel slag.

4. Conclusions

In this paper, a new process of preparing SSUP in the laboratory is proposed. The differences in soundness and cementitious activity between SSUP and SSP were also studied. The conclusions of this study are drawn as follows:

- (1) The process of preparing SSUP in the laboratory involves grinding it with a horizontal ball mill for 50 min, then mixing it evenly with grinding aids at a ratio of 75 g/1 mL and grinding it with a planetary ball mill for 15 min. The D15 particle size of obtained SSUP is 0.479 μm , D50 particle size is 2.031 μm , D90 particle size is 12.191 μm , 30 μm sieve size is 0.08%, and specific surface area is 4.13 m^2/g . By comparing the microstructure of SSUP and SSP by SEM, it can be concluded that the particle size distribution of SSUP is more uniform and the surface is rougher.
- (2) The water requirement of normal consistency decreases with the increase in SSUP and SSP dosage. When the dosage is 15% and 30%, the water consumption of SSP is higher than that of SSUP, while when the dosage is 45% and 60%, the water consumption of SSUP is higher than that of SSP.
- (3) The soundness of SSUP with different dosages is better than that of SSP. When the dosage increases from 15% to 60%, the difference in the distance between the tip of the Lehigh clamp pointer of SSUP increases from 0.10 mm to 0.75 mm, while that of SSP increases from 1.00 mm to 6.65 mm.

- (4) The results of the hydration heat experiment show that the hydration degree and rate of SSUP are better than those of SSP. The 7 d and 28 d activity indexes of SSUP are higher than those of SSP. At 7 d, the activity index of SSUP is 65.61%, 13.63% higher than that of SSP. The activity index of SSUP at 28 d is 94.19%, 24.57% higher than that of SSP. The XRD test results show that, with the augment of hydration time, the relative contents of C₃S, C₂S, C₃A, and C₂F crystals in SSUP and SSP gradually decrease, while the relative contents of C-S-H gel gradually increase and the increase in C-S-H gel and in SSUP is greater.

Author Contributions: Conceptualization, S.W.; Data curation, M.C.; Formal analysis, Y.S.; Funding acquisition, M.C.; Investigation, Y.S.; Methodology, D.C., S.L. and X.Z.; Supervision, M.C.; Writing—original draft, Y.S.; Writing—review & editing, D.C., S.L. and X.Z. All authors have read and agreed to the published version of the manuscript.

Funding: This work was supported by the Research Project of Wuhan University of Technology Chongqing Research Institute, YF2021-01. The authors gratefully acknowledge their financial supports.

Institutional Review Board Statement: Not applicable.

Informed Consent Statement: Not applicable.

Data Availability Statement: Not applicable.

Conflicts of Interest: The authors declare no conflict of interest.

References

1. Ali, S.; Iqbal, S.; Room, S.; Ali, A.; Rahman, Z.U. Value added usage of granular steel slag and milled glass in concrete production. *J. Eng. Res.* **2021**, *9*, 73–85. [[CrossRef](#)]
2. Wang, Q.; Yang, J.; Yan, P. Cementitious properties of super-fine steel slag. *Powder Technol.* **2013**, *245*, 35–39. [[CrossRef](#)]
3. Aikawa, Y.; Shinobe, K.; Ueda, Y.; Nito, N.; Sakai, E. Analysis of hydration of blast furnace slag in high-volume blast furnace slag cement using an expanded hydration equation. *J. Ceram. Soc. Jpn.* **2018**, *126*, 109–114. [[CrossRef](#)]
4. Chindapasirt, P.; Jaturapitakkul, C.; Sinsiri, T. Effect of fly ash fineness on microstructure of blended cement paste. *Constr. Build. Mater.* **2007**, *21*, 1534–1541. [[CrossRef](#)]
5. Li, Q.L.; Chen, M.Z.; Liu, F.; Wu, S.P.; Sang, Y. Effect of superfine blast furnace slag powder on properties of cement-based materials. *Mater. Res. Innov.* **2015**, *19*, S168–S171. [[CrossRef](#)]
6. Fang, M.; Fang, G.; Xia, Y.; Wang, H.; IOP Publishing. In Study on Compressive Strength of Concrete Mixed by Steel Slag Powder and Fly Ash. In Proceedings of the 6th International Conference on Energy Materials and Environment Engineering (ICEMEE), Electr Network, Hulun Buir, China, 28–30 August 2020.
7. Zhang, L.; Wang, Q.; Zheng, Y.; Cang, Z.; Gisele, K.; Yu, C.; Cang, D. Synergistic effect and mechanism of waste glass on the mechanical properties and autoclave stability of cementitious materials containing steel slag. *Constr. Build. Mater.* **2021**, *311*, 125295. [[CrossRef](#)]
8. Chen, W.; Huo, Z.; Yang, Z.; IOP Publishing. In Study on the Performance of Green Cement with Large Amount of Steel Slag Addition. In Proceedings of the International Conference on Construction, Aerotropolis, Aviation and Environmental Engineering (ICCAE), Taoyuan, Taiwan, 14–16 May 2019.
9. He, W.; Zhao, J.; Yang, G. Investigation on the Role of Steel Slag Powder in Blended Cement Based on Quartz Powder as Reference. *Adv. Civ. Eng.* **2021**, *2021*, 5547744. [[CrossRef](#)]
10. Guo, J.; Bao, Y.; Wang, M. Steel slag in China: Treatment, recycling, and management. *Waste Manag.* **2018**, *78*, 318–330. [[CrossRef](#)]
11. Zhu, G.; Hao, Y.; Xia, C.; Zhang, Y.; Hu, T.; Sun, S. Study on cementitious properties of steel slag. *J. Min. Metall. Sect. B-Metall.* **2013**, *49*, 217–224. [[CrossRef](#)]
12. Hu, S.; Wang, H.; Zhang, G.; Ding, Q. Bonding and abrasion resistance of geopolymeric repair material made with steel slag. *Cem. Concr. Compos.* **2008**, *30*, 239–244. [[CrossRef](#)]
13. Wang, G.; Wang, Y.; Gao, Z. Use of steel slag as a granular material: Volume expansion prediction and usability criteria. *J. Hazard. Mater.* **2010**, *184*, 555–560. [[CrossRef](#)] [[PubMed](#)]
14. Li, J.; Zhao, S.; Song, X.; Ni, W.; Mao, S.; Du, H.; Zhu, S.; Jiang, F.; Zeng, H.; Deng, X.; et al. Carbonation Curing on Magnetically Separated Steel Slag for the Preparation of Artificial Reefs. *Materials* **2022**, *15*, 2055. [[CrossRef](#)] [[PubMed](#)]
15. Zhou, Y.; Ji, Y.; Zhang, Z.; Ma, Z.; Gao, F.; Xue, Q.; Xu, Z. Effect of acid-activation on CaO existential state and reactive properties of hot-splashed steel slag in cement-based materials. *Struct. Concr.* **2022**, 1464–4177. [[CrossRef](#)]
16. Liu, F.; Chen, M.Z.; Li, F.Z.; Li, Q.L.; Wu, S.P.; Sang, Y. Effect of ground steel slag powder on cement properties. *Mater. Res. Innov.* **2015**, *19*, S150–S153. [[CrossRef](#)]
17. Zhu, X.; Hou, H.; Huang, X.; Zhou, M.; Wang, W. Enhance hydration properties of steel slag using grinding aids by mechanochemical effect. *Constr. Build. Mater.* **2012**, *29*, 476–481. [[CrossRef](#)]

18. Liu, S.; Li, L. Influence of fineness on the cementitious properties of steel slag. *J. Therm. Anal. Calorim.* **2014**, *117*, 629–634. [[CrossRef](#)]
19. Shi, Y.; Chen, H.; Wang, J.; Feng, Q. Preliminary investigation on the pozzolanic activity of superfine steel slag. *Constr. Build. Mater.* **2015**, *82*, 227–234. [[CrossRef](#)]
20. Zhang, T.; Yu, Q.; Wei, J.; Li, J. Investigation on mechanical properties, durability and micro-structural development of steel slag blended cements. *J. Therm. Anal. Calorim.* **2012**, *110*, 633–639. [[CrossRef](#)]
21. Cao, L.; Shen, W.; Huang, J.; Yang, Y.; Zhang, D.; Huang, X.; Lv, Z.; Ji, X. Process to utilize crushed steel slag in cement industry directly: Multi-phased clinker sintering technology. *J. Clean. Prod.* **2019**, *217*, 520–529. [[CrossRef](#)]
22. Li, X.; Liu, T.; Ouyang, J.; Yang, H. In Mechanochemical processing of ultrafine steel slag powders. In Proceedings of the 2nd International Conference on Advanced Materials and Its Application (AMA 2013), Wuhan, China, 16–19 May 2013; pp. 211–215.
23. Hu, S.G.; He, Y.J.; Lu, L.N.; Ding, Q.J. Effect of fine steel slag powder on the early hydration process of Portland cement. *J. Wuhan Univ. Technol.-Mater. Sci. Ed.* **2006**, *21*, 147–149. [[CrossRef](#)]
24. Ma, W. Effect of steel slag powder on cement road performance. *Highw. Transp. Inn. Mong.* **2021**, *2021*, 7–9+26.
25. Wang, L.; Long, H.-m.; Zeng, H. Effect of Composite Grinding Aid on Steel Slag Ultrafine Powder. *China Metall.* **2019**, *29*, 75–79.
26. Zhou, M.; Cheng, X.; Chen, X. Studies on the Volumetric Stability and Mechanical Properties of Cement-Fly-Ash-Stabilized Steel Slag. *Materials* **2021**, *14*, 495. [[CrossRef](#)] [[PubMed](#)]
27. Liao, J.; Zhang, Z.; Ju, J.; Zhao, F. In Comparative analysis of steel slag characteristics and treatment process. In Proceedings of the 3rd International Conference on Materials and Products Manufacturing Technology (ICMPMT 2013), Guangzhou, China, 27–28 February 2014; pp. 378–384.
28. Wang, Q.; Yan, P.; Han, S. The influence of steel slag on the hydration of cement during the hydration process of complex binder. *Sci. China-Technol. Sci.* **2011**, *54*, 388–394. [[CrossRef](#)]
29. Yang, J.; Lu, J.; Wu, Q.; Xia Ming, F.; Li, X. Influence of steel slag powders on the properties of MKPC paste. *Constr. Build. Mater.* **2018**, *159*, 137–146. [[CrossRef](#)]